Shubnikov—de Haas experiments on potassium-hydrogen graphite intercalation compounds (KH_x-GIC's)

T. Enoki,* N.-C. Yeh, S.-T. Chen, and M. S. Dresselhaus
Department of Physics, Massachusetts Institute of Technology, Cambridge, Massachusetts 02139
(Received 19 August 1985)

Potassium-hydrogen-graphite ternary compounds (KH_x-GIC, $0<x<1$) are donor-type compounds containing an ionic intercalant K^+H^-. Basically the effect of hydrogen addition is the uptake of electrons from the potassium so that fewer electrons are available for conduction in the graphite π bands. To obtain Fermi-surface information directly, Shubnikov—de Haas (SdH) measurements were carried out on stage-1, -2, and -4 KH_x-GIC's. The results are compared with the electronic properties of K-GIC's and KHg_x-GIC's. The observed oscillations are qualitatively modeled using the three-dimensional dilute-limit model. These Fermi-surface results are related to other experiments on KH_x-GIC's, such as magnetic susceptibility, electronic specific heat, Raman scattering, and superconductivity. For example, it is found that because of the strong electron affinity of hydrogen, the charge transfer to hydrogen and graphite in stage-2 KH_x-GIC's completely depletes the electrons in the potassium conduction band, consistent with the experimental specific-heat results. The basic conclusion that the uptake of hydrogen results in a lower electron concentration in the graphite π bands is supported by all experiments.

I. INTRODUCTION

Potassium hydride KH is an ionic insulator, in which the charge transferred from the K atoms is localized on hydrogen atoms to form hydride anions H^-. This is in contrast to the hydrogen in transition-metal or rare-earth metal hydrides, where metallic alloys are formed between the metal and hydrogen atoms (e.g., PdH_x), such that the strong interactions between the hydrogen and conduction electrons of the metal delocalize part of the negative-charge cloud surrounding the hydrogen atoms.[1] In the case of potassium-hydrogen graphite intercalation compounds (KH_x-GIC's),[2–6] where the chemical formula is $C_{4n}KH_x$ for the stage $n=1,2$ compounds,[7] the volume per hydrogen of the intercalate alkali-metal sandwich containing the layer of hydrogen atoms is larger than the corresponding volume of the transition-metal hydrides. Thus for the KH_x-GIC's, there is sufficient room for the electronic cloud to be located around the hydrogen atoms. A physical limitation to the maximal hydrogen uptake in these compounds is the number of electrons that can be transferred from the potassium conduction bands, while leaving sufficient charge behind to bond the GIC. These negatively-charged hydrogen atoms are screened from the graphitic conduction electrons by the positively-charged potassium layers.[8–11] Consequently to first approximation, most of this charge localization remains around the hydrogen layers in the intercalation compounds. Thus we can expect the electronic properties of KH_x-GIC's to be different from those of K-GIC's and KHg_x-GIC's. Recent electronic specific-heat studies[12] on hydrogen-chemisorbed stage-2 C_8KH_x indicated a reduction of the electronic density of states at the Fermi level $N(E_F)$ as the hydrogen uptake increased, consistent with a competition of the graphite and hydrogen layers for electrons from the potassium layers.

The phonon modes of the KH_x-GIC's are also of interest and different from those of the alkali-metal donor compounds. For example, the Raman line for the E_{2g_2} graphite mode in stage-1 KH_x-GIC's exhibits a Raman mode at 1596 cm^{-1} which is higher than typical alkali-metal donor GIC's,[13,14] consistent with the above arguments on charge transfer. The Lorentzian line shape for the stage-1 KH_x-GIC's is in sharp contrast to the Breit-Wigner line shape for the stage-1 alkali-metal GIC's,[14] indicating a much weaker interaction between the graphite and the intercalate. Recent magnetic susceptibility measurements[15,16] are also consistent with the idea that the hydrogen layers in the KH_x-GIC's obtain electrons from the other constituents of the compound, in contrast to the charge transfer behavior in K-GIC's. Furthermore, although enhancement of superconductivity was found in hydrogen-chemisorbed C_8K (with stoichiometry $C_8KH_{0.19}$),[17] no superconductivity has been observed in stage-2 KH_x-GIC samples having hydrogen uptake $x\sim0.67$.[18] This behavior can be compared with the remarkable increase in the transition temperature T_c for the stage-1 KHg_x-GIC's upon addition of small concentrations of hydrogen, consistent with a decrease in the charge transfer to the graphite π bands and an increase in the density of states at the Fermi level.[19]

Shubnikov—de Haas (SdH) measurements were undertaken to obtain more direct information on the Fermi surface of KH_x-GIC's in order to account for the observed electronic and lattice mode properties of these compounds. Because of the strong electron affinity of hydrogen, one may expect the uptake of hydrogen to result in weaker coupling between the intercalate and graphite bounding layers as well as a reduction of available electrons in graphitic π bands relative to the corresponding

alkali-metal GIC's. The results of the present Shubnikov—de Haas study on KH_x-GIC's (where $x \sim 0.8$) show that this simple concept is generally valid.

II. SYNTHESIS AND STRUCTURAL CHARACTERIZATION

KH_x-GIC's were prepared by the direct KH intercalation method,[7,20] using both highly oriented pyrolytic graphite (HOPG) and Kish graphite single-crystal host materials. The typical size of HOPG-based samples is about $6 \times 2.5 \times 0.1$ mm^3. The Kish graphite based samples have irregular shapes and have generally a similar size, typically $3 \times 3 \times 0.1$ mm^3. For the intercalation, the host graphite materials and dried KH powder were sealed together in a Pyrex glass tube at a pressure of 10^{-5}—10^{-6} Torr, and the mixture was then heated isothermally at constant temperature for 7 to 10 days. The intercalation temperatures were $410 \geq T \geq 350$ °C and $210 \geq T \geq 200$ °C for stage-1 and stage-2 samples, respectively. The KD_x-GIC's were also prepared under the same conditions as the corresponding KH_x-GIC's. These samples were characterized for stage index and stage fidelity using x-ray (00l) diffraction, and the interplane distances were determined to be 8.56, 12.08 (or 11.93 Å, see next section), and 18.81 Å for stage-1, stage-2, and stage-4 KH_x-GIC's, respectively (see Fig. 1). With regard to ordering along the c axis, the KH_x-GIC's are isostructural with respect to the KHg_x-GIC's.[21] Pure stage-2 samples were obtained, but the stage-1 samples were found to contain small admixtures of stage-2 regions, even though the samples were intercalated for sufficiently long times to produce single-staged compounds without stage-2 species. The in-plane structures were determined[22,23] by (hk0) electron diffraction patterns taken with a transmission electron microscope (TEM); $(2\times2)R0°$ and $(\sqrt{3}\times\sqrt{3})R30°$ phases are found in both stage-1 and stage-2 KH_x-GIC's and KD_x-GIC's. These in-plane structures are found to be similar to those reported for stage-1 KHg_x-GIC's.[24]

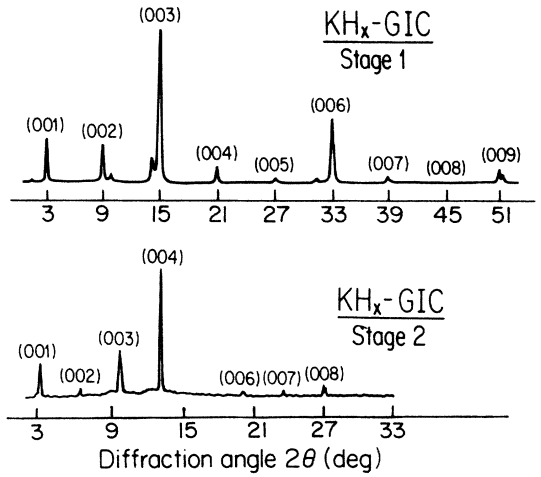

FIG. 1. (00l) x-ray diffraction spectra of stage-1 and stage-2 KH_x-GIC's taken with a Mo x-ray source.

III. EXPERIMENTAL DETAILS

Sample handling was carried out in an Ar glove bag to protect these air sensitive KH_x-GIC's. After each sample was mounted on a mica sheet, electrical contacts were made using silver paint following the geometrical arrangement of Montgomery.[25] After mounting, the samples were placed in rectangular glass tubes which were then sealed using epoxy after filling them with about 650 Torr of Ar, 100 Torr of H_2, and 10 Torr of He. This gas mixture suppressed the desorption of hydrogen and provided good heat exchange between the samples and the heat bath in the magnetoresistance experiment at liquid-helium temperatures.

The magnetoresistance was measured by a dc method. To determine the Shubnikov—de Haas oscillatory frequencies and the angular dependence of these frequencies, we used a rotation device which provided a wide range of angles θ between the c axis of the sample and the magnetic field $\mathbf{H}$. The rotation device was designed to fit within a one-inch bore Bitter magnet, which provided magnetic fields up to 23 T. The angular dependence was studied by rotating the sample around the direction of the current $\mathbf{I}$ such that $\mathbf{I} \perp \mathbf{H}$ for all θ. Thus the transverse magnetoresistance was measured in all cases. Data acquisition was carried out using a MINC computer, and digital processing of data was done to obtain the Fourier power spectra of the resistance versus $1/H$. Thus, we obtained the frequencies of the SdH oscillations which are directly related to the extremal Fermi-surface (FS) cross sections.

To determine the effective masses of our samples, we used a specially designed insert for controlling the temperatures from 4.2 to 40 K. This insert required a larger bore of two inches, so that the Bitter magnetic used for the effective-mass studies provided magnetic fields only up to 19 T. We therefore determined the effective masses for various frequencies by examining the oscillatory amplitudes as a function of temperature. After the SdH experiments were completed, we verified that the staging of the samples had not changed, using (00l) x-ray diffraction scans.

IV. RESULTS

Figure 2 shows typical Shubnikov—de Haas (SdH) results for the transverse magnetoresistance (ρ) for stage-1, -2, and -4 KH_x-GIC's at 4.2 K. In each case ρ depends quadratically on H at low fields ($H \ll 1$ T), characteristic of closed orbits perpendicular to the field direction in a metal, while quantum oscillations dominate the high-field region of each trace. The nonoscillatory component of the magnetoresistance was subtracted from the observed data to extract the oscillatory components before taking the Fourier transform. The Fourier transform of the SdH spectrum for a stage-1 KH_x-GIC 1.4 K is shown in Fig. 3(a) which exhibits three SdH frequencies $\nu_\alpha = 30$ T, $\nu_\beta = 106$ T, and $\nu_\gamma = 647$ T that are summarized in Table I. One of these stage-1 samples shows the highest frequency at $\nu_\delta \sim 4000$ T which is going to be discussed later. Also included in Table I are SdH frequencies for K-GIC's and KHg_x-GIC's. The same experiments were also performed on the stage-1 KD_x-GIC's, and the observed SdH

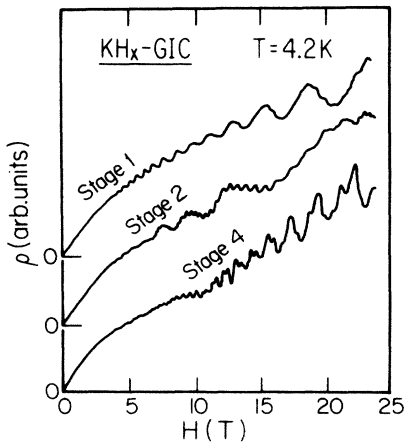

FIG. 2. Typical traces of Shubnikov–de Haas oscillations for stage-1, -2, and -4 KH_x-GIC's at 4.2 K.

frequencies were found to be consistent with those of the stage-1 KH_x-GIC's. This confirms the idea that the replacement of hydrogen by its isotope deuterium in the KD_x-GIC's does not change the electronic properties.

The results on seven stage-1 samples which were used in these experiments were classified into two types A and B, each exhibiting the same frequencies but relatively different amplitudes and temperature dependences (see Fig. 4). The Shubnikov–de Haas traces for sample type A exhibited a stronger temperature dependence [Fig. 4(A)], while those for sample type B showed a weaker temperature dependence [Fig. 4(B)]. The amplitude of the oscillation β was small for type A, but fairly large for type B, while the amplitude of the oscillation γ was larger for type-A samples. Moreover, the nonoscillatory magnetoresistance of sample A was larger than that of the B samples.

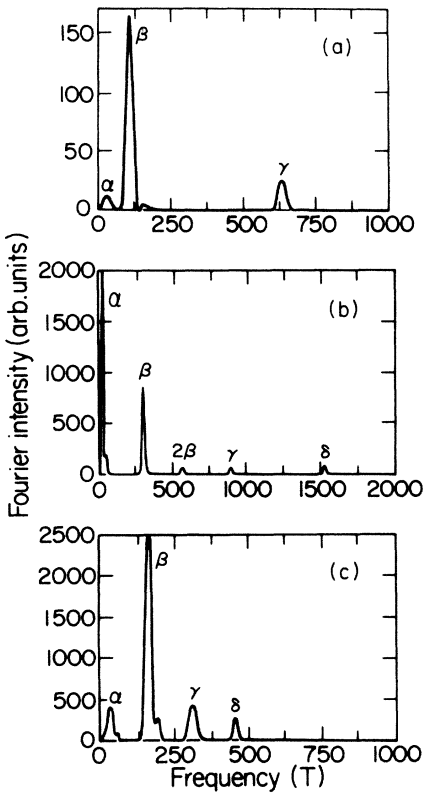

FIG. 3. The Fourier transform power spectra of the Shubnikov–de Haas oscillations for (a) the stage-1 KH_x-GIC, (b) the stage-2 KH_x-GIC, and (c) the stage-4 KH_x-GIC. The various SdH frequencies are labeled on each figure (see Table I).

The amplitude of SdH oscillation A_i is given by the following equation:[26]

$$|A_i(T)| \propto T \exp[-2\pi^2 k_B (T+T_D)/\hbar\omega_i] , \quad (1)$$

TABLE I. Characteristic frequencies of SdH oscillations for stage-1 and stage-2 KH_x-GIC's. The frequencies for C_8K, $C_{24}K$, and KH_x-GIC from the literature are also shown (Refs. 24 and 28–30).

Compound	Stage 1	Stage 2	Stage 4
KH_x-GIC's	4000±20 T (δ)	1525±20 T (δ)	461±17 T (δ)
	647±20 T (γ)	763±30 T (γ)	309±26 T (γ)
	106±13 T (β)	283±25 T (β)	164±22 T (β)
	30±10 T (α)	41±20 T (α)	32±26 T (α)
KHg_x-GIC's	2490 T (γ)	1490 T (ν)	
	1090 T (β)	1250 T (δ)	
	52 T (α)	1119 T (λ)	
		901 T (μ)	
		221 T (γ)	
		199 T (β)	
		28 T (α)	
K-GIC's	2870 T	439 T	354 T
		306 T	276 T
		282 T	264 T
		149 T	150 T
		133 T	132 T
			24 T
			12 T

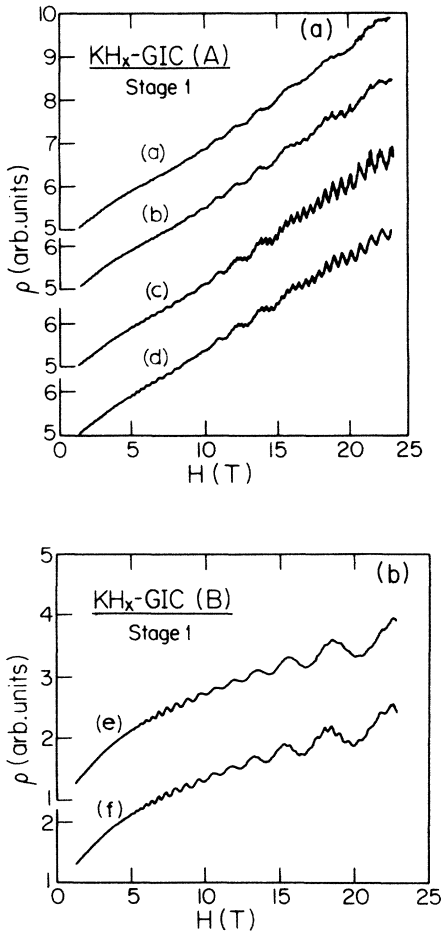

FIG. 4. Shubnikov—de Haas oscillations for two types of stage-1 KH_xGIC's samples. Traces for A-type samples are for (a) 4.2 K, $\theta=0°$; (b) 2.0 K, $\theta=0°$; (c) 1.4 K, $\theta=0°$; and (d) 1.4 K, $\theta=10°$, respectively; and those for type-B samples are for $\theta=0°$ and (e) 4.2 K and (f) 1.4 K.

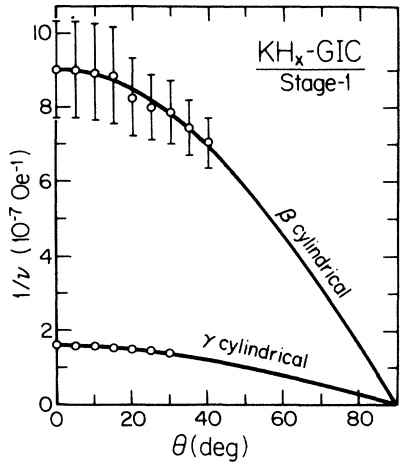

FIG. 5. Angular dependence of the Shubnikov—de Haas oscillations β and γ for the stage-1 KH_x-GIC. The solid lines are the fits for cylindrical Fermi surfaces.

where ω is the cyclotron frequency and $\omega_i=eH/m_i^*c$, H is the magnitude of the applied magnetic field, and m_i^* is the cyclotron effective mass of the electrons associated with Fermi surface i. The Dingle temperature T_D is related to the collision time $\tau_{\rm col}$ of carriers with defects by $T_D=\hbar/\pi k_B\tau_{\rm col}$. The values of T_D estimated for the oscillation α from Eq. (1) were determined to be 0.4 and 5.1 K for samples A and B, respectively. As mentioned above, the stage-1 samples include some admixture of a stage-2 constituent; these admixtures are expected to vary from sample to sample, are position dependent within a sample, and are highly sensitive to the synthesis conditions. The difference in the scattering process is attributed to the variety and concentration of defects in these two types of stage-1 samples. At present we have no detailed information on the microstructural differences between the type-A and type-B samples, nor do we know how these microstructural differences affect the scattering mechanism. However, we do not attribute these differences in SdH behavior to stage-2 admixtures since the frequencies of the SdH oscillations for the stage-2 KH-GIC (presented below) are different from those observed for the stage-1 samples.

The angular dependence of SdH oscillations β and γ is shown in Fig. 5, and the solid line is the fit of the angular dependence to a cylindrical Fermi surface. This strong anisotropic character of the Fermi surface is reminiscent of graphitic energy bands, though measurements to much larger angles θ are necessary to determine departures from a cylindrical Fermi surface. The cyclotron effective masses of stage-1 KH_x-GIC's associated with oscillations α and β were determined from the temperature dependence of the SdH amplitudes (see Fig. 6) through the following formula:

$$\frac{m_i^*}{m_e}=-\frac{\ln(A_i/T)}{T}\frac{\hbar eH_0}{2\pi^2k_Bm_ec}=-(|S|/14.694)H_0\ , \tag{2}$$

where m_e is the free-electron mass, S is the slope (in K^{-1}) of a plot of $\ln(A_i/T)$ versus T, while A_i is the amplitude

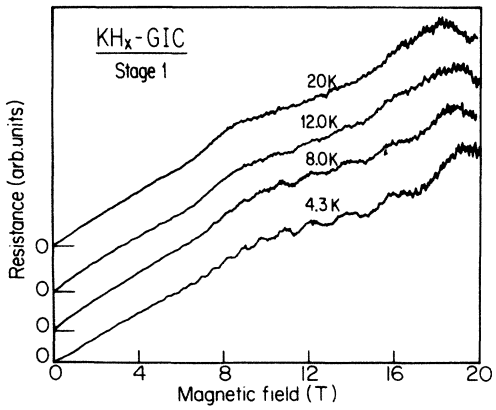

FIG. 6. Traces for SdH oscillations of stage-1 KH_x-GIC's for various temperatures.

(in arbitrary units) of the SdH oscillations, and H_0 is the magnetic field (in units of tesla) where we make the amplitude measurements. The effective masses are thus determined from a plot of $\ln(A_i/T)$ versus T as shown in Fig. 7(a) for the stage-1 samples, yielding $m_\alpha=0.046m_e$ and $m_\beta=0.23m_e$.

The magnetoresistance for the stage-2 KH_x-GIC's shown in Fig. 2 exhibits four oscillatory components. The frequencies of these components were estimated to be $\nu_\alpha=41$ T, $\nu_\beta=283$ T, $\nu_\gamma=763$ T, and $\nu_\delta=1525$ T, respectively [Fig. 3(b)]. The frequencies taken on six stage-2 KH_x-GIC samples are summarized in Table I. It is found that there is no difference within experimental error in the oscillations between the samples with interplane distance $I_c=12.08$ Å and $I_c=11.93$ Å. The temperature dependence of the SdH oscillations at liquid-helium temperatures for the stage-2 KH_x-GIC's exhibits anomalous behavior in two respects, as shown in Fig. 8. Firstly, with decreasing temperature, the intermediate frequency oscillation β vanishes below about 2 K, though the lower-frequency oscillation α does not show an anomalous temperature dependence. Furthermore, the magnetoresistance for the stage-2 compound exhibits a nonlinear behavior, insofar as the amplitudes of the two high-frequency oscillations β and γ are strongly enhanced relative to the α oscillation by application of a high current. This nonlinear effect can be seen in Fig. 8 by comparing the traces taken with a small current [15 mA for traces (b)—(e)] to trace (a) taken with a current of 70 mA. These phenomena need further investigation.

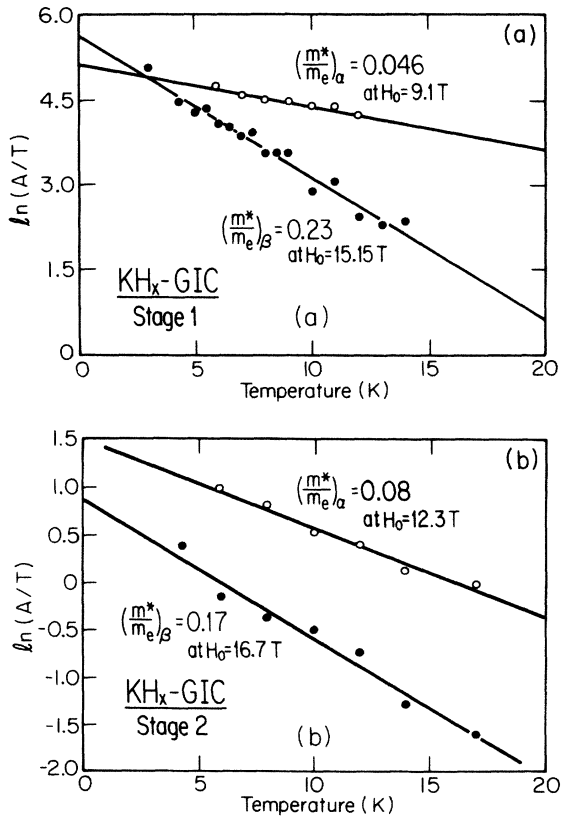

FIG. 7. Effective masses determined from the temperature dependence of the SdH oscillations α and β in (a) stage-1 KH_x-GIC's and (b) stage-2 KH_x-GIC's.

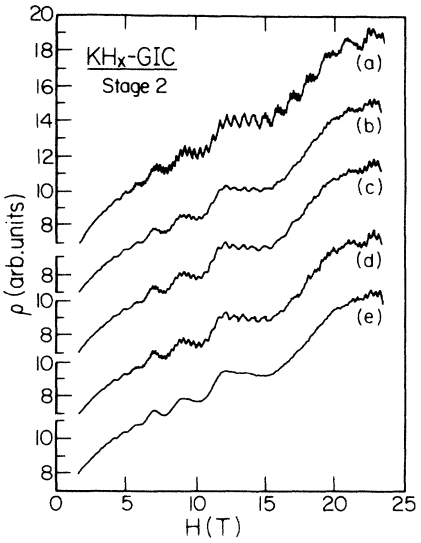

FIG. 8. Traces for the Shubnikov—de Haas oscillations for the stage-2 KH_x-GIC at various temperatures. (a) 4.2 K with an applied current of 70 mA, (b) 4.2 K, (c) 3.0 K, (d) 2.2 K, and (e) 2.0 K. The applied current for traces (b)—(e) is 15 mA.

Analysis of the temperature dependence of the oscillations α and β for the stage-2 compounds yields $m_\alpha=0.08m_e$ and $m_\beta=0.17m_e$, as shown in Fig. 7(b).

The magnetoresistance for the stage-4 KH_x-GIC yields four SdH frequencies: $\nu_\alpha=32$ T, $\nu_\beta=164$ T, $\nu_\gamma=309$ T, and $\nu_\delta=461$ T, as shown in Table I.

V. DILUTE LIMIT MODEL ANALYSIS

Because of the presence of hydrogen and its strong electron affinity in the KH_x-GIC's, the electrons available for the graphite π bands are reduced substantially as compared with the situation in K-GIC's and KHg_x-GIC's. Therefore it can be argued that the dilute-limit model provides a better approximation for the analysis of the SdH frequencies in KH_x-GIC's than for K-GIC's and KHg_x-GIC's. We thus assume that the graphite band parameters can be used to describe the graphite π bands in the KH_x-GIC's without substantial change in their values. The Fermi energy E_F is chosen as a fitting parameter for the maximal experimental frequencies, and then the c-axis zone-folding technique is applied to calculate the other frequencies[27,28] using the expression for the graphite energy bands:

$$\mathcal{A}^e_{\max}=(4\pi/3a_0^2\gamma_0^2)(E_3-E_F)(E_2-E_F)/(1+2\gamma_4/\gamma_0)^2$$
$$=2\pi e\nu_{\max}/\hbar c\ , \qquad (3)$$

where $\mathcal{A}^e_{\max}$ is the maximal Fermi-surface cross section observed, a_0 is the graphite in-plane lattice constant 2.46 Å,

$$E_2=\Delta-\gamma_1\Gamma+0.5\gamma_5\Gamma^2\ ,$$

and $E_3=0.5\gamma_2\Gamma^2$, where Δ and the γ_i's are graphite band

TABLE II. Comparison between the observed SdH frequencies (ν_{obs}) and calculated SdH frequencies (ν_{calc}) from the three-dimensional dilute-limit model for stage-1, -2, and -4 KH_x-GIC's. All frequencies are in units of tesla. (NO indicates that the frequencies were not observed, and NE indicates that no SdH frequencies were expected.)

Stage 1		Stage 2		Stage 4	
ν_{obs}	ν_{calc}	ν_{obs}	ν_{calc}	ν_{obs}	ν_{calc}
(4000)	NE	1525	1525	461	461
647	647	NA	1334	NO	419
106	367	763	865	309	309
30	161	283	383	164	161
		41	NE	32	NE

parameters,[27] $\Gamma=2$ (for the cross section around the K point), and ν_{max} is the maximal SdH oscillatory frequency observed from experiments.

The comparison between the calculated and observed frequencies is tabulated in Table II for stage-1, -2, and -4 compounds. Good agreement is obtained for the SdH frequencies for stage-4, but for stage-1 and stage-2, the agreement is not as good. Using this simple model, the Fermi energies for various stages can be estimated to be ~ 0.65, ~ 1.15, and ~ 0.49 eV for stage-1, -2, and -4 KH_x-GIC's, respectively (see Table III).

The cyclotron effective masses can also be calculated from this model using the relation

$$m_i^* = (\hbar^2/2\pi)(\partial \mathcal{A}_i/\partial \varepsilon)\,|\,E_F\ , \tag{4}$$

where $\mathcal{A}_i$ is the ith Fermi cross-sectional area enclosed by the orbit in the plane normal to H. We can use Eq. (3) and the E_F values given above to determine $\mathcal{A}_i$. In this analysis we substitute $\Gamma_j = 2\cos(c_0 j/I_c)$ and $2(\gamma_4/\gamma_0)\cos(c_0 j/I_c)$ for Γ and $2(\gamma_4/\gamma_0)$ respectively to obtain the various cross sections, pertaining to the Fermi surface at the edge of the folded Brillouin zone, where $j=0,1,2,\ldots$. Thus m_i^* (i represents various oscillations α, β, γ, etc.) can be estimated for the various SdH frequencies of the stage-1 and stage-2 KH_x-GIC's. The calculated results using Eq. (4) and the experimental results from Fig. 7 are compared and tabulated in Table IV for both stage-1 and stage-2 compounds. Again, we obtained qualitative agreement between the calculated and experimental results. Notice that the light effective masses are reminiscent of graphitic masses, lending support to our original approximation of using graphitic bands with graphite band parameters and the zone-folding technique. To obtain a better model for the lower stage compounds ($n=1,2$), we need to take the intercalant-graphite coupling into account instead of using an "empty intercalant" model as is done above.

VI. DISCUSSION

One of the most important pieces of information obtained from SdH experiments is the charge transfer to the graphite π bands (f_C) per carbon atom, which can be obtained using the following formula assuming a cylindrical Fermi surface:

$$f_C = \sum_i (2\pi g_s g_c \mathcal{A}_i/I_c)/(8nV_{BZ})\ , \tag{5}$$

where g_s is the spin degeneracy, g_c is the number of cylinders in each folded Brillouin zone, having volume V_{BZ}, and n is the stage index. (In our case, both g_s and g_c are equal to 2.) Once the charge transfer f_C to the graphite π bands is determined, we can find the charge transfer from each potassium atom f_K by using the approximation that for the hydrogen atoms $f_H=-1$, and taking the hydrogen uptake to be $x\sim 0.8$ for both stage-1 and stage-2 KH_x-GIC's in accordance with the work of Guérard *et al.*[7] We also chose the $(2\times 2)R0°$ structure as the dominant in-plane phase.[14,22] The f_K values can thus be calculated using the following formula:

$$f_K = 4n\,|f_C| + x\,|f_H|\ , \tag{6}$$

TABLE III. The fractional charge transfer coefficients f_C, f_K (or f_{KHg}), and f_H on the C, K (or KHg), and H atoms are tabulated in units of charge per atom. The density of states at the Fermi level $N(E_F)$ is in units of states/eV atom of C.

GIC	f_C	f_H	f_K (or f_{KHg})	E_F (eV)	$N(E_F)$
$C_4KH_{0.8}$	−0.020	−1	+0.88	0.65	0.24
$C_8KH_{0.8}$	−0.033	−1	+1	1.15	0.06
C_4KHg_x	−0.094[a]		+0.38	1.53[a]	
C_8KHg_x	−0.064[a]		+0.51	1.0[a]	
C_8K	−0.075[b]		+0.6	1.4[b]	
$C_{24}K$	−0.042[c]		+1		

[a]Reference 24.
[b]Reference 29.
[c]Reference 31.

TABLE IV. The comparison between calculated (calc) effective masses and observed (obs) effective masses in stage-1 and stage-2 KH_xGIC's.

	$(m^*/m_e)_{obs}$	$(m^*/m_e)_{calc}$
Stage-1 α	0.046	0.056
β	0.23	0.13
Stage-2 α	0.08	0.13
β	0.17	0.15

where the stoichiometry is $C_{4n}KH_x$. The charge transfer values determined in this way are listed in Table III. Comparing these values to those in K-GIC's (Refs. 27–31) and KHg_x-GIC's (Ref. 24), we found that the f_C values in KH_x-GIC's are substantially less than those in the other two donor-GIC's indicating a major reduction of electron concentration in the graphite π bands because of the presence of hydrogen, which has a high electron affinity.

The upper limits of both the Fermi energy E_F and the charge transfer f_C can also be crudely estimated by assuming complete charge transfer from potassium atoms and full intercalation of hydrogen, i.e., $f_K=+1$ and $x\sim 0.8$. This gives $(E_F)_{max}\sim 0.90$ eV, $(f_C)_{max}\sim 0.050$ for stage-1, and $(E_F)_{max}\sim 0.87$ eV, $(f_C)_{max}\sim 0.025$ for stage-2 KH_x-GIC's, respectively. Thus we can conclude that the f_C and E_F values we obtained from SdH experiments are within a reasonable range.

There is, however, another possibility which has to be considered for stage-1 KH_x-GIC's. Because of the limitation of the available upper magnetic field and of the quality of the samples in these SdH experiments, one may not exclude the possibility of the existence of another higher SdH frequency. If this were true, then we could assign the observed highest frequency 647 T to be the second oscillation ν_1, and use Eq. (3) to estimate the Fermi energy. This gives $E_F=0.89$ eV, $\nu_{max}=2070$ T, and $f_C=0.045$, which are also reasonable values. The observation of a SdH frequency of 4000 T on one occasion on one stage-1 sample is suggestive of the possibility that there may be SdH frequencies higher than ~ 650 T. Also suggestive of the possibility of a higher SdH frequency for the stage-1 compounds is the stage dependence of f_C which (see Table III) is opposite in sign to that of the other donor intercalates (e.g., K and KHg) or to simple charge transfer concepts.

Using the f_C and f_K values for KH_x-GIC's in Table III and adopting the concept of a rigid-band model,[12,32] we can estimate the density of states at the Fermi level $N(E_F)$ using the following procedure. Assuming two-dimensional graphitic π bands for the graphite electrons and three-dimensional free-electron bands for the potassium conduction electrons, we write the following expressions for the carrier concentrations and densities of states:

$$n_C=2nn_u(f_K-x)=\int_0^{E_F} dE\, N_G(E)\ , \tag{7}$$

$$n_K=2n_u(1-f_K)=\int_\delta^{E_F} dE\, N_S(E)\ , \tag{8}$$

$$N_G(E)=8nE/(\pi I_C D^2)\ , \tag{9}$$

$$N_S(E)=\sqrt{E-\delta}(2m_s^*/\hbar^2)^{3/2}/\pi^2\ , \tag{10}$$

$$E_G(k)=Dk\ , \tag{11}$$

where $D=(\sqrt{3}/2)\gamma_0 a_0$, and m_s^* is the effective mass for the three-dimensional (3D) bands, so that the total density of states at the Fermi level becomes

$$N(E_F)=[(dn_C/dE)\,|_{E_F}+(dn_K/dE)\,|_{E_F}]/8n_u n$$
$$=u(f_K-x)^{1/2}+v(1-f_K)^{1/3}\ , \tag{12}$$

in which u and v are given by

$$u=3^{1/4}a_0/(n\pi^{1/2}D)\ , \tag{13}$$

$$v=(3^{2/3}m_s^* a_0^{4/3}I_c^{4/3})/[(2\pi)^{4/3}\hbar^2 n]\ , \tag{14}$$

where n_C is the concentration of electrons in the graphite π bands, n_K is the concentration of nearly free electrons left in the potassium band, n_u is the number of unit cells per unit volume, δ is the energy at the bottom of the three-dimensional potassium band, and $N(E_F)$ is the density of states at the Fermi level (in units of states/eV atom of C). The $N(E_F)$ values thus obtained are 0.24 states/eV atom of C for stage-1 and 0.06 states/eV atom of C for stage-2 KH_x-GIC's, respectively. From the electronic specific-heat measurements[12] on hydrogen chemisorbed stage-2 KH_x-GIC's with $x\sim 0.65$, the density of states $N(E_F)$ was found to be ~ 0.2 states/eV atom of C if the electron-phonon enhancement is neglected. If we extrapolate the plot of $N(E_F)$ versus x given in Ref. 12 to $x\sim 0.8$ by assuming a linear decrease in $N(E_F)$ with increasing hydrogen uptake x, we obtain a value $N(E_F)$ of ~ 0.14 states/eV atom of C, though the errors in this estimate are large. Comparing this value to the $N(E_F)$ estimated from SdH experiments (see Table III), we obtain the electron-phonon coupling constant λ to be 1.33. A better estimate for λ from specific-heat measurements gives $\lambda=0.87$ for $x=0.65$,[12] which is in agreement with SdH results within experimental errors. A large electron-phonon coupling constant may be consistent with theoretical predictions, suggesting that the interpocket and intrapocket electron-phonon interactions add to give a large value of λ.[33] The comparison between the present SdH results and the specific-heat results implies that an increase in the intercalated hydrogen concentration in the stage-2 C_8KH_x compounds reduces the concentration of donated electrons to the graphite π bands.

The reduction of the concentration of donated electrons results in a suppression of the coupling between the electrons in the graphite bounding layers and those in the intercalate layers. This reduced coupling is consistent with the Lorentzian line shape of the Raman line for the stage-1 KH_x-GIC's (in contrast to the Breit-Wigner line shape for the stage-1 K-GIC's), and with the anomalously high frequencies of the E_{2g_2} mode compared to that for other stage-1 donor GIC's.[13,27]

The $N(E_F)$ determined from the SdH results also relates to the magnetic susceptibility measurements[15] since

$$\chi_{total}=\chi_{core}+\chi_{Pauli}+\chi_{orbital}+\chi_{ls}\ , \tag{15}$$

where the Pauli contribution is given by $\chi_{Pauli}=\mu_B^2 N(E_F)$,

the core contribution χ_{core} is known, and the functional form of the localized spin contribution χ_{ls} can be estimated from ESR measurements,[34] which is shown to be small compared with the total susceptibility.[15,16] Thus we can obtain χ_{orbital} from measurements of the total magnetic susceptibility χ_{total}. For $\mathbf{H}||c$ axis, the functional form of the temperature-dependent orbital susceptibility is found to be[15]

$$\chi_{\text{orbital}}=a_1+a_2/(T+a_3) \tag{16}$$

(where $a_1>0$, $a_2<0$, and $a_3>0$) for both stage-1 and stage-2 KH_x-GIC's.[16] This result is reminiscent of a combination of the McClure magnetic susceptibility (χ_{McClure}),[35,36] which is valid for graphite, and the Landau-Peierls magnetic susceptibility ($\chi_{\text{L-P}}$),[37,38] which is valid for donor K-GIC's. The magnetic susceptibility results also indicate that the presence of the hydrogen layer reduces the carrier concentration in the graphite. The stage dependence of the susceptibility shows that the hydrogen layer exhibits acceptor behavior in an otherwise donor GIC. This is consistent with the SdH experimental results. A further study of this point is in progress.

The absence of superconductivity in stage-2 KH_x-GIC's (for $x>0.65$) (Ref. 18) is in contrast to the presence of superconductivity in C_8K ($T_c=0.15$ K) and the enhancement of superconductivity by hydrogen addition to obtain $C_8KH_{0.19}$ ($T_c=0.22$ K).[17] The absence of superconductivity is consistent with the absence of K conduction electrons from the SdH results (see Table III). The theoretical model for superconductivity in the alkali-metal donor GIC's requires the coexistence of both graphitic π electrons and intercalant s electrons.[39] The presence of superconductivity in GIC's can thus be correlated with the partial occupation of the intercalate bands.[40–44] In the case of stage-1 KH_x-GIC ($x\sim0.8$), the $f_C=-0.020$ value obtained from SdH measurements leaves open the possibility of incomplete charge transfer from the potassium bands, where $f_K=+0.88$. No superconductivity has been observed in this compound up to the present time. This may be due to a T_c value lower than the measured temperature range. It is also likely to have an empty potassium s band (i.e., $f_K=+1$) if we do not exclude the possibility for the existence of higher SdH frequencies in stage-1 samples. Furthermore, the coexistence of graphitic and s electrons may not be a sufficient condition for the presence of superconductivity in donor GIC's. More theoretical and experimental work may be necessary for further understanding of this point.

Finally, we would like to discuss the anomalous temperature dependence of the amplitude of the SdH oscillation for stage-2 KH_x-GIC's. Figures 8 and 9 show the temperature dependence of the amplitudes for the oscillations α and β. For the lower-frequency oscillation α, we see that $\ln(A/T)$ increases with decreasing temperature in a normal manner, while the β frequency shows an abrupt anomalous decrease in $\ln(A/T)$ below about 2 K. There has been one report of an anomalous temperature dependence of the SdH oscillations for the longitudinal magnetoresistance of Bi, where the amplitude decreases with decreasing temperatures.[45] This effect was explained by a phonon-assisted inter-Landau level scattering mechanism.[46] This phenomenon in stage-2 KH_x-GIC's is under further investigation.

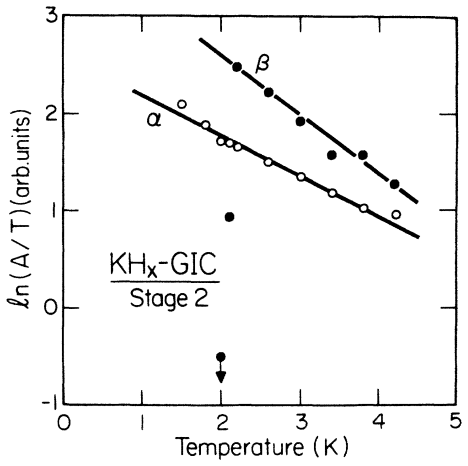

FIG. 9. Temperature dependence of the amplitude A for the SdH oscillations α and β in the stage-2 KH_x-GIC plotted as $\ln(A/T)$ vs T. Notice that in contrast to the temperature dependence shown in Fig. 8, in the lower-temperature range (from 4.2 K down to 1.3 K), the β oscillation exhibits an anomalous behavior below $\sim$2.2 K.

VII. SUMMARY

The observation of Shubnikov–de Haas frequencies provides a powerful method for obtaining information on the electronic structure of GIC's. The SdH experiments were done on a number of stage-1, -2, and -4 KH_x-GIC ($x\sim0.8$) samples to investigate the electronic structures of these materials. KH_x-GIC's are believed to be isostructural to KHg_x-GIC's with the intercalant layers consisting of K-Hg-K sandwich layers. The in-plane superlattices exhibit both $(2\times2)R0°$ and $(\sqrt{3}\times\sqrt{3})R30°$ structures.

$\nu_\alpha=30$ T, $\nu_\beta=106$ T, and $\nu_\gamma=647$ T in stage-1, $\nu_\alpha=41$ T, $\nu_\beta=283$ T, $\nu_\gamma=763$ T, and $\nu_\delta=1525$ T in stage-2, and $\nu_\alpha=32$ T, $\nu_\beta=164$ T, $\nu_\gamma=309$ T, and $\nu_\delta=461$ T in stage-4 KH_x-GIC's. (See Table I.) The energy state associated with the hydrogen $1s$ orbital is well below E_F because of the large electron affinity of hydrogen. Therefore the available electrons in the graphite π bands are substantially reduced in KH_x-GIC's relative to K-GIC's and KHg_x-GIC's. The three-dimensional dilute-limit model based on the graphite band parameters was used to interpret the electronic structures of these KH_x-GIC's. The model works qualitatively for describing both the observed frequencies and cyclotron effective masses. The charge transfer to graphite (e^-/atom of C) was determined to be $f_C=-0.020$ for stage-1 and $f_C=-0.033$ for stage-2 KH_x-GIC's. Since a hydrogen grabs one electron from a potassium donor atom, the stage-2 KH_x-GIC is found to have complete charge transfer from potassium ($f_K=1$),

consistent with the experimental results for the low-temperature electronic specific heat. The complete charge transfer also explains the absence of superconductivity for the stage-2 KH_x-GIC.

Values of the density of states $N(E_F)$ were calculated from f_C values by adopting the idea of a rigid-band model, and the values which were obtained are $N(E_F)=0.24$ states/eV atom of C for stage-1 and $N(E_F)=0.06$ states/eV atom of C for stage-2. Since χ_{Pauli} can be obtained from $N(E_F)$, the orbital magnetic susceptibility ($\mathbf{H}||c$ axis) was found to contain both Landau-Peierls and McClure contributions, showing that the presence of hydrogen in the intercalate layers of KH_x-GIC's exhibits acceptorlike behavior in a GIC which would normally be donorlike.

ACKNOWLEDGMENTS

The authors would like to thank Dr. G. Dresselhaus, Dr. K. Sugihara, Dr. H. Inokuchi, Dr. H. Suematsu, Dr. Y. Yoshida, and Dr. I. Tsujikawa for their helpful discussions. We are also grateful to A. Antonious and Dr. G. Roth for their technical assistance. This work was supported by U.S. Air Force Office of Scientific Research (AFOSR) Grant No. F49620-83-C-0011, except for T.E. who acknowledges supported by U.S. Department of Energy (DOE) Grant No. DE-AC02-83ER45041 and the Japanese Ministry of Education, Science and Culture. All the experiments were done at the Francis Bitter National Magnet Laboratory, under support by the National Science Foundation.

*Permanent address: Institute for Molecular Science, Okazaki 444, Japan.

[1]G. Alefeld and J. Vöckl, *Hydrogen in Metals* (Springer, Berlin, 1978).
[2]D. Saehr and A. Hérold, Bull. Soc. Chim. 3130 (1965).
[3]M. Colin and A. Hérold, Bull. Soc. Chim. 1982 (1971).
[4]P. Lagrange, A. Metrot, and A. Hérold, C. R. Acad. Sci. **278**, C701 (1974).
[5]P. Lagrange, M. H. Portman, and A. Hérold, C. R. Acad. Sci. **283**, C557 (1976).
[6]D. Guérard, P. Lagrange, and A. Hérold, Mater. Sci. Eng. **31**, 29 (1977).
[7]D. Guérard, C. Takoudjou, and F. Rousseaux, Synth. Metals **7**, 43 (1983).
[8]G. Furdin, P. Lagrange, A. Hérold, and C. Zeller, C. R. Acad. Sci. **282**, C563 (1976).
[9]T. Enoki, H. Inokuchi, and M. Sano, Chem. Phys. Lett. **86**, 285 (1982).
[10]T. Enoki, M. Sano, and H. Inokuchi, J. Chem. Phys. **78**, 2017 (1983).
[11]T. Trewern, R. K. Thomas, G. Naylor, and J. W. White, J. Chem. Soc. Faraday Trans. 1 **78**, 2369 (1982).
[12]T. Enoki, M. Sano, and H. Inokuchi, Phys. Rev. B **32**, 2497 (1985).
[13]N. C. Yeh, T. Enoki, L. McNeil, L. Salamanca-Riba, M. Endo, and G. Dresselhaus, *Extended Abstracts 1984 Fall Meeting of Materials Research Society, 1984,* edited by P. C. Eklund, M. S. Dresselhaus, and G. Dresselhaus (Materials Research Society, Pittsburgh, PA, 1984), p. 246.
[14]M. S. Dresselhaus and G. Dresselhaus, *Light Scattering in Solids III,* Vol. 51 of *Topics in Applied Physics,* edited by M. Cardona and G. Güntherodt (Springer, New York, 1982), p. 3.
[15]N. C. Yeh, T. Enoki, L. Salamanca-Riba, and G. Dresselhaus, *Extended Abstracts of the 17th Biennial Conference on Carbon, Lexington, 1985,* edited by P. J. Reucroft and P. C. Eklund (American Carbon Society and the University of Kentucky, Lexington, KY, 1985), p. 194.
[16]N. C. Yeh and G. Dresselhaus (unpublished).
[17]S. Kaneiwa, M. Kobayashi, and I. Tsujikawa, J. Phys. Soc. Jpn. **51**, 2375 (1982).
[18]M. Sano, H. Inokuchi, M. Kobayashi, S. Kaneiwa, and I. Tsujikawa, J. Chem. Phys. **72**, 3840 (1980).
[19]G. Roth, A. Chaiken, T. Enoki, N. C. Yeh, G. Dresselhaus, and P. M. Tedrow, Phys. Rev. B **32**, 533 (1985).
[20]D. Guérard, C. Takoudjou, and F. Rousseaux, *Proceedings of the 6th London International Carbon and Graphite Conference, London, 1982* (Society of the Chemical Industry, London, 1982), p. 85.
[21]P. Lagrange, M. Makrini, D. Guérard, and A. Hérold, Synth. Metals **2**, 191 (1980).
[22]L. Salamanca-Riba, N. C. Yeh, T. Enoki, M. Endo, and M. S. Dresselhaus, *Extended Abstracts of Fall Meeting of Materials Research Society, Boston, 1984,* edited by P. C. Eklund, M. S. Dresselhaus, and G. Dresselhaus (Materials Research Society, Pittsburgh, PA, 1984), p. 249.
[23]L. Salamanca-Riba, N. C. Yeh, M. Endo, M. S. Dresselhaus, and T. Enoki (unpublished).
[24]G. Timp, T. C. Chieu, P. D. Dresselhaus, and G. Dresselhaus, Phys. Rev. B **29**, 6940 (1984).
[25]H. C. Montgomery, J. Appl. Phys. **42**, 2971 (1971).
[26]E. N. Adams and T. D. Holstein, J. Phys. Chem. Solids **10**, 254 (1959).
[27]M. S. Dresselhaus and G. Dresselhaus, Adv. Phys. **30**, 139 (1981).
[28]G. Dresselhaus and S. Y. Leung, Solid State Commun. **35**, 819 (1981).
[29]S. Tanuma, H. Suematsu, K. Higuchi, R. Inada, and Y. Onuki, in *Proceedings of the Conference on the Application on High Magnetic Fields in Semiconductor Physics,* edited by J. F. Ryan (Clarendon, Oxford, 1978), p. 85.
[30]K. Higuchi, H. Suematsu, and S. Tanuma, J. Phys. Soc. Jpn. **48**, 1532 (1980).
[31]G. Dresselhaus, S. Y. Leung, M. Shayegan, and T. C. Chieu, Synth. Metals **2**, 321 (1980).
[32]K. Sugihara (private communication).
[33]H. Kamimura (private communication).
[34]T. Enoki, H. Inokuchi, and M. Sano (private communication).
[35]J. W. McClure, Phys. Rev. **104**, 666 (1956).
[36]J. W. McClure, Phys. Rev. **108**, 612 (1957).
[37]F. J. Disalvo, S. A. Safran, R. C. Haddon, and J. V. Waszczak, Phys. Rev. B **20**, 4883 (1979).
[38]S. A. Safran and F. J. Disalvo, Phys. Rev. B **20**, 4889 (1979).
[39]R. Al-Jishi, Phys. Rev. B **28**, 112 (1982).
[40]M. G. Alexander, D. P. Goshorn, D. Guérard, P. Lagrange, M. El Makrini, and D. G. Onn, Synth. Metals **2**, 203 (1980).

[41]Y. Koike and S. Tanuma, J. Phys. Soc. Jpn. **50**, 1964 (1981).
[42]L. A. Pendrys, R. Wachnik, F. L. Vogel, P. Lagrange, G. F. Furdin, M. El Makrini, and A. Hérold, Solid State Commun. **38**, 677 (1981).
[43]Y. Iye and S. Tanuma, Phys. Rev. B **25**, 4583 (1982).
[44]Y. Iye and S. Tanuma, Synth. Metals **5**, 257 (1983).
[45]S. Tanuma, Phys. Condens. Matter **19**, 95 (1975).
[46]S. Tanuma and R. Inada, Suppl. Prog. Theor. Phys. **57**, 231 (1975).